JOURNAL OF OPTOELECTRONICS AND ADVANCED MATERIALS, Vol. 11, No. 9, September 2009, p. 1175 - 1181

Characterisation of the internal structure and local optical properties of thick layers of hydroxyapatite by Coherence Probe Microscopy♣

P.C. MONTGOMERY*, D. MONTANER, L. PRAMATAROVA[a] AND E. PECHEVA[a]
Institut d'Electronique du Solide et des Systèmes (InESS), Laboratoire commun ULP-CNRS, UMR 7163, 23 rue du Loess, 67037 Strasbourg, France.
[a] *Institute of Solid State Physics, Bulgarian Academy of Sciences, 72 Tzarigradsko Chaussee Blvd., 1784 Sofia, Bulgaria.*

Thick transparent or semi-translucent layers are of growing importance in several key scientific and technological fields such as microelectronics, nanotechnology and biomaterials. New characterisation tools are required to cope with the complexity of these new materials and with the large range of scales involved (nm, µm, mm). In this paper, we report work on the development of new optical imaging instrumentation for characterising such layers, based on scanning white light interferometry. We demonstrate that as well as being able to measure surface roughness and shape, scanning interferometry can also be used to measure the local effective refractive index, reflectivity spectra and internal structure, using point Z-scanning and 2D cross sectional profiling. Results are shown for thin diamond-like carbon layers on polycarbonate and thick layers of hydroxyapatite.

(Received November 5, 2008; accepted December 15, 2008)

Keywords: Thick films, Topography, Optical properties, Coherence Probe Microscopy

1. Introduction

Thick transparent or semi-translucent layers are of growing importance not only in semiconductors but also in optics, chemistry and biomaterials. Characterisation of such layers becomes challenging because of the high thickness (tens of µm), the structural complexity, the inhomogeneity and/or the presence of pores. In the case of classical materials such as SiO_2, the chemical and optical properties are well known, and the challenge is to analyse the topography of buried structures. However, in biomaterials such as the growth of hydroxyapatite (HA) layers from solution, neither the topography nor the optical properties are known, and they can vary considerably according to the growth conditions [1]. There is thus a growing need for new analysis tools for characterising such complex materials, to add to the information available from classical techniques. For example, near field probe techniques such as AFM (atomic force microscopy), while useful for high resolution surface characterisation, are not well adapted to large fields (greater than 10 µm) or depths (greater than 2µm). SEM is time consuming and destructive. Confocal microscopy does not provide spectroscopic information.

What is required is the ability to probe large areas (>100 µm) and to be able to extract different types of information (topographic, internal structure, optical…) locally on a submicron scale. Far field imaging, combined with advanced modes and image processing, is proving very promising for such work, even leading to a new field of microscopy, known as "Nanoscopy" [2]. For example, in Coherence Probe Microscopy (CPM) the use of white light scanning interferometry allows nm axial resolution and the rapid measurement of high roughness over large areas (fields of up to 2.5 mm without scanning) [3-5].

In previous work, we demonstrated how CPM can be used to characterise simple structures buried under thick transparent layers [6]. This paper extends the use of CPM to the characterisation of more complex layers that may contain buried layers, cavities or delaminated regions. The Z-scan mode that we have developed allows manual scanning of the multiple peak fringe envelope pattern along Z, to provide further information concerning buried structures. Local measurements of the effective refractive index of small particles can be performed. Results are demonstrated on the delamination and buckling of thin DLC (diamond-like carbon) layers on polycarbonate, and on complex thick layers of HA.

2. White light interferometry analysis of transparent layers

♣ Paper presented at the International School on Condensed Matter Physics, Varna, Bulgaria, September 2008

The techniques developed are based on white light scanning interferometry (WLSI), which is also known as Coherence Probe Microscopy (CPM). In this section, we describe the classical use of CPM in surface roughness measurement and develop the different ideas for new measurement modes possible with this technique, that are particularly useful in thick layer characterisation.

2.1. White light interferometry theory

The 3D measurement of surfaces using interference microscopy is typically based on the use of an optical interference microscope equipped with an interference objective of the Michelson, Mirau, or Linnik type [7]. A translation table is used to perform the Z-scan of the fringes over the depth of the sample, and a sequence of images is digitized. Measurement is based on the processing and analysis of the interference fringes resulting from the recombination between the light reflected by the sample and that reflected by the reference mirror. The light intensity I measured in a white light interferometer that is spatially incoherent can be approximated by the following form:

$$I(x,y,z) = \sum_{\lambda_1}^{\lambda_2} I_0(x,y,z)[1 + R \cdot \Gamma(\Delta L)\cos(\phi(x,y,z))] \tag{1}$$

The x and y coordinates correspond to the image coordinates, and the z coordinate indicates the axial location of the sample surface. The quantity I_0 is an offset related to the reference and object beam intensities. The interferogram envelope function Γ is related to the spectral profile of the white light, and R is the effect of the reflection coefficient on the sample. Detection of the peak of the fringe intensity or the fringe envelope at a pixel, over the depth scanned determines, the position of the surface at that point. Measuring this for every pixel in the camera array defines a non-contacting, virtual optical probe plane of nm thickness, that when scanned over the depth of the sample enables small and large roughnesses to be quantified.

Many techniques for extracting the surface position have been proposed in the literature. These include demodulation, correlation, determination of the barycentre of the envelope, Fourier, Hilbert and wavelet techniques, phase shifting, peak fringe scanning microscopy (PFSM), and determination of the peak of the fringe visibility, or the five sample adaptive algorithm (FSA) [8].

Several different measurement modes exist, typically the greyscale image (quantitative data), the 3D image (qualitative view), and 2D profiles. An extended depth of field is also available in the reflection mode, by adding together the maximum intensity values at each pixel [9]. Advanced commercial software exists for exploiting the quantitative data in surface roughness analysis.

CPM is a complimentary technique to near field microscopy, and has certain advantages because of the use of an optical probe. In applications in which a lateral resolution of 0.4 µm is sufficient, CPM is much more versatile than near field probes. The use of a nanometrically thin optical probe plane in CPM allows nm axial sensitivity over very large depths (100 µm in our system, several mm with appropriate scanning tables). Commercial systems quote vertical sensitivities of better than 0.1 nm and RMS repeatabilities of 0.01 nm, but in practice these values are very sample dependent. Because mechanical scanning only needs to be performed along one axis (Z), real time 3D scanning speeds can be attained, leading to 4D microscopy [10]. The use of polychromatic light also allows spectroscopic techniques to be used [8].

On the other hand, it is important to understand the limits of the technique, to avoid or correct errors and artefacts in certain types of measurement. For example, measurements are limited to surface slopes within the numerical aperture of the objective (less than 72° for NA = 0,95). In measuring step heights between different materials, errors of up to 30 nm can occur due to the phase change on reflection resulting from differences between the complex refractive indices [11]. Other artefacts can also occur, such as the widening of high narrow structures such as those found in MEMS. In [12] we demonstrated how these artefacts can be considerably reduced by optimising the optical system.

As new and more complex materials are investigated, there is a growing need for the development of simulation tools for studying the optical probe in CPM and its interaction with different surfaces and interfaces. New signal and image processing algorithms are also required to extract the useful information. Work is being carried out in both of these fields at InESS, and will be published in the future.

While the use of a physical probe in near field microscopy leads to the main advantage of nm lateral resolution in these techniques, this also leads to a fundamental limitation; that of being restricted to surface characterisation. On the contrary, with CPM the use of an optical probe allows such investigation of buried layers. The Z-scan mode that we introduced [1] allows manual investigation of buried structures and 2D cross sectional profiling. These are now described.

The technique for characterising thick layers with CPM consists first of scanning the interference fringes over the full depth of the sample and storing a series of images XY at fixed intervals in order to build up an image stack XYZ. For ease of analysis, the reference mirror is slightly tilted to give horizontal fringes in the XY images. The software we have developed then allows different types of characterisation, which are now detailed.

2.2. "Z-scan" point analysis technique of thick layers

The "Z-scan" technique consists of selecting a pixel (or area of pixels and averaging the intensity to reduce noise) at the required position in an XY image, in order to observe the fringe signal along Z at that point. Different processing tools are available in order to extract the fringe envelope and make measurements of the thickness and refractive index. The envelope is found using a rectification and low pass filtering algorithm and the automatic peak detector function, to detect the peaks.

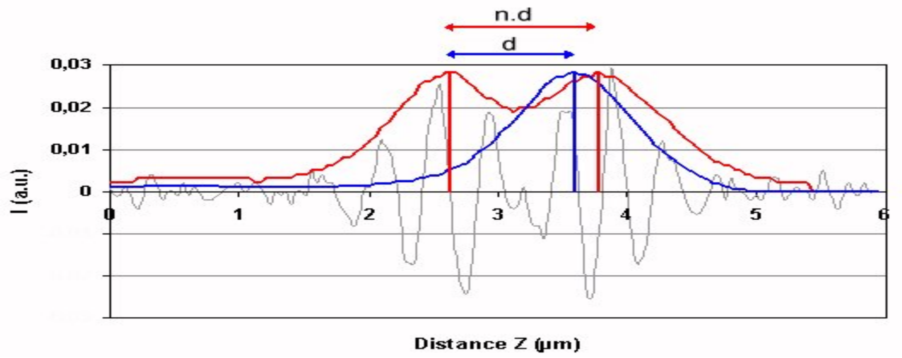

Fig. 1. Example of Z-scan measurement of the local refractive index.

For example, selection of a point on the bare substrate gives the position along Z at that point from the peak of the single envelope (blue curve in Fig. 1). Selection of a point on a transparent layer (red curve in Fig. 1) on the same line X (same fringe) leads to a double fringe envelope. The position of the peak of the air/layer surface gives the thickness of the layer, when compared to the position of the substrate. The second peak gives the position of the layer/substrate buried interface. The distance between the two peaks (red curve), ΔZ, gives the optical path through the layer, where:

$$\Delta Z = n_{eff}.d \qquad (2)$$

Knowing ΔZ and d, the local effective refractive index at that point can be calculated:

$$n_{eff} = \Delta Z/d \qquad (3)$$

2.3. 2D profile sectioning by image processing of thick layers

A cross sectional profile can be produced by processing a given XZ image from the XYZ stack (see Fig. 9(a) for example). In this case, more efficient 2D image processing is used on the XY image, to isolate the fringe envelopes. A sliding window 2D filter is used to smooth the fringes, the length of the envelope along Z and 3 to 5 pixels wide along X, to remove noise. A 1D peak detection function is then applied along Z, to identify the envelope peaks and a choice of image processing functions is available to highlight the cross sectional profile. In the simplest case of a single transparent layer, in the presence of two peaks, these can be identified and labelled with different colours.

2.4. White light scanning interferometry system

The CPM system developed at InESS has been described elsewhere [3-7].

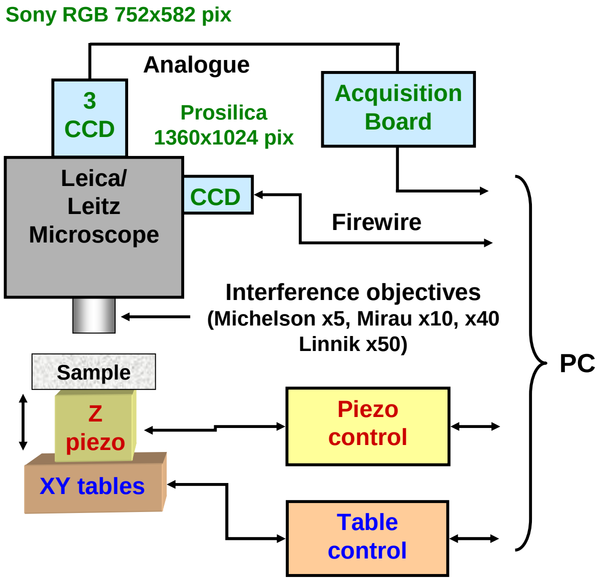

Fig. 2. Experimental system layout for analysing thick transparent layers.

In brief, it consists of two metallographic reflection microscopes equipped with Michelson, Mirau or Linnik Interference objectives (Fig. 2). Either a high resolution monochrome CCD camera (digital "Firewire" connection) or a three target RGB CCD are used for imaging. Vertical scanning is performed with a capacitive feedback piézo, having a range of 100 µm and a sensitivity of 1 nm.

CPM is typically used for the measurement of high surface roughness, such as the laser processed steel surface shown in Fig. 3, as used for nanostructuring before hydroxyapatite growth in the laser-liquid-solid-interaction

(LLSI) technique [1]. The method is quick, precise and versatile for quantifying surface roughness.

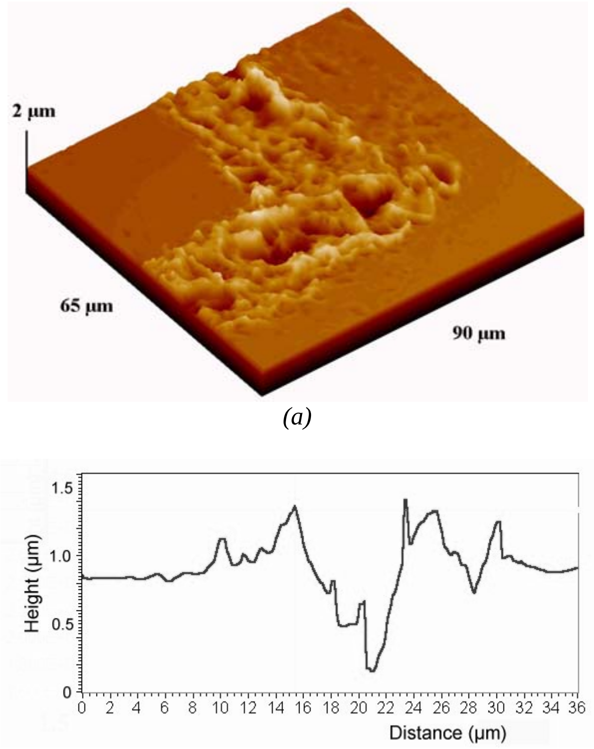

(a)

(b)

Fig. 3. Typical results using CPM to measure the surface roughness of a laser processed steel substrate : (a) 3D view; (b) Line profile.

The measurement of larger microelectronic structures, such as the coil on a CMOS chip, is shown in Fig. 4.

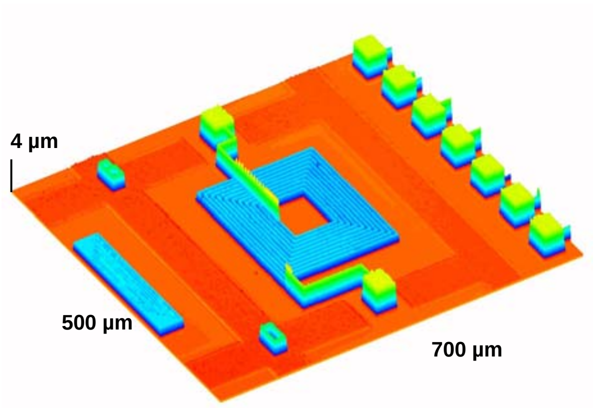

Fig. 4. Typical results using CPM to measure the 3D shape of a miniature CMOS coil.

3. Single layer analysis

In the course of measuring different opto- and micro-electronic materials and samples, more recently we have faced the challenge of characterising thick transparent layers with CPM. While imaging ellipsometry [13] is very good for mapping the layer thickness and optical parameters with diffraction limited lateral resolution, the technique is limited to the characterisation of thin films (< 1 µm). CPM has the advantage of being able to be used on much thicker samples.

Amongst others, the layers we have had to characterise are thin (60 nm) DLC layers on polycarbonate [14], resin diffractive optical elements [15], CMOS structures under silicon oxide or nitride, planarising layers of FOx ("flowable oxide") on ceramics for photovoltaics [16], thick layers (<30 µm) of hydroxyapatite on various substrates and colloid layers on glass and ZnSe (in the study of sorption of heavy metals in soils). To illustrate how CPM can be used to contribute more information than just roughness, some results are now given on the thin DLC layers and thick HA layers.

3.1. DLC layers on polycarbonate

Thin transparent films less than 500 nm thick are not easy to characterise with CPM, because of the difficulty of separating the two overlapping fringe envelopes. However, when such thin films delaminate, it is possible to extract useful information concerning adherence. For example, during trials with the plasma deposition of thin (typically 60 nm) diamond-like carbon (DLC) layers [14] on polycarbonate substrates, the internal stress under certain conditions leads to a "buckling" of the layer and the formation of hollow "bubbles" of DLC.

An example of such a structure is shown in Fig. 5(a), consisting of a direct reflection image. This "bubble" structure in fact continued to grow outwards in size over a period of a few minutes in free air, as the DLC layer delaminated and different "bubbles" coalesced.

The fringes observable near to the edges of the "bubble" structure are not due to the interference objective, since the image was taken in the direct reflection mode. They are Newton's fringes due to the optical wedge structure formed by the DLC layer and the substrate.

By measuring the 3D shape of such "bubbles" of DLC with CPM (Fig. 5(b)), they were found to be between 2 µm and 3 µm in height. Under other growth conditions, wavy strings of such "bubbles" could be seen to form in random "worm-like" structures.

The more interesting information came from the 2D profiles of such structures (Fig. 5(c)) and the observation of the position of the measured DLC/substrate interface (blue curve) compared with that of the air/DLC surface (red curve).

Under certain growth conditions, the measured interface (blue curve) was found to be at the same height as that of the neighbouring substrate, leading to an optical path Δz equal to that of the "bubble" height, d (equation (2)). In this case, with a refractive index equal to 1, it can be concluded that the DLC has lifted straight off the substrate at this point, without adhering. Under other growth conditions, for the case illustrated (Fig. 5(c)), the DLC/substrate interface (blue curve) can be observed to be below that of the neighbouring substrate, with Δz > d. The most plausible explanation for such a measurement is that the DLC has sufficient adherence to the polymer substrate at this point to be able to tear away with it a small thickness of polycarbonate, leaving a slight depression.

Such information concerning the 3D form of delaminated structures and of the degree of adherence of the DLC layers has been useful in the development of new plasma deposition techniques.

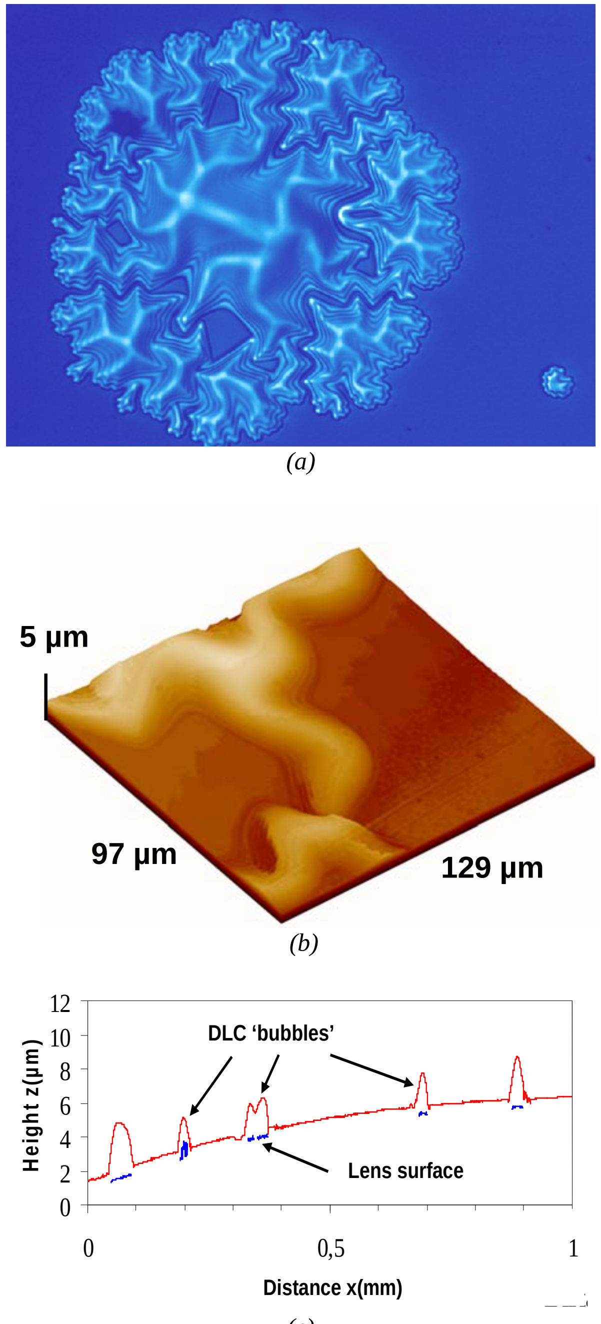

(a)

(b)

(c)

Fig. 5. CPM analysis of "bubbles" of DLC delaminating from a polycarbonate substrate due to internal stress: (a) Reflection image of a large area; (b) 3D image of part of a "bubble"; (c) 2D profile of several "bubbles".

4. Characterisation of thick layers of hydroxyapatite

Man-made layers of HA, the basic constituent of bone, teeth and shells, plays a vital role at the interface between alloys and bone in human implants. The ISSP (BAS, Sofia, Bulgaria) have developed a novel laser assisted technique (LLSI) for growing thick layers of HA in a solution of simulated body fluid [17].

Studies have been carried out on different types of substrate (stainless steel, silicon, titanium, glass…) and on the effects of laser assisted growth, nanostructuring of the substrate and the inclusion of nanodiamonds [17]. Many techniques have been employed to characterise these samples, such as TEM (transmission electron microscopy), SEM (scanning electron microscopy), AFM, XRD (X-ray diffraction), FTIR (Fourier transform IR spectroscopy) and Raman spectroscopy. CPM has been found to be very useful for quantifying the surface roughness, the general aspect and some of the local properties, at a microscopic scale.

4.1. Surface roughness

While SEM gives a general view of the aspect of HA layers, the results are not always quantitative and the layers degrade easily under the influence of a high energy electron beam.

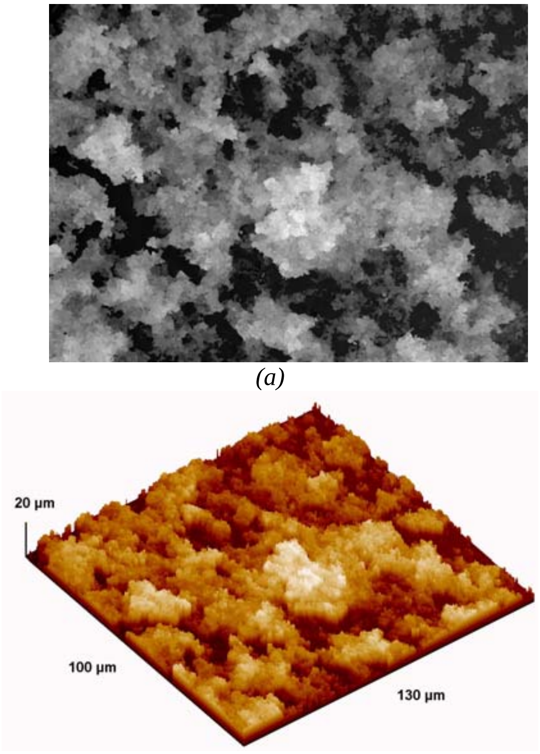

(a)

(b)

Fig. 6. Typical results using CPM to measure the 3D roughness of a thick hydroxyapatite layer on steel: (a) Greyscale image (quantitative data); (b) 3D image (qualitative view).

Classical stylus profiling cannot be used, because the tip tends to dig into the layer. AFM can be used for small roughnesses (less than 2 µm) but not for larger roughnesses up to 20 µm, because of the restricted dynamic range. Spectroscopic ellipsometry gives incorrect results because of the high layer thickness and the presence of pores.

Using an optical probe, CPM is well suited for measuring such thick layers. The aspect of the roughness (Fig. 6(a)) is very similar to that found with SEM, but has the advantage of being quantified, providing a quick tool for characterizing the roughnesses of different samples [1].

4.2. Z-scan point depth characterisation

Further investigation has been possible using the "Z-scan" technique for analyzing the internal structure of the thick layers [1]. The drawing in Fig. 7(a) is a model of the layer resulting from scanning different points. A typical Z-scan is shown in Fig. 7(b), the peaks marked with numbers corresponding to the different surfaces and interfaces in 7(a). A uniform transparent layer was detected from the peaks 1 and 2, and is clearly visible as a uniform set of double fringes in the XZ image. This was identified as being a SiO_2 layer on the Si substrate. The peak 4 corresponds to the air/HA surface, and subsequent peaks in between (N° 3) correspond to cavities within the layer. In this way, it is possible to better understand the internal structures of such thick layers.

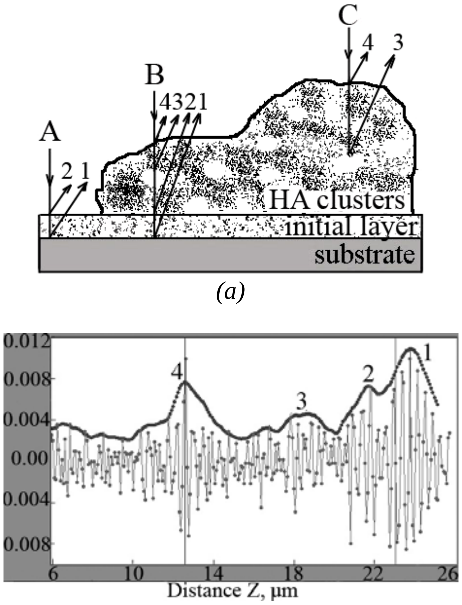

(a)

(b)

Fig. 7. Z-scan results on a thick hydroxyapatite layer: (a) Model of the hydroxyapatite layer; (b) Fringe signal from B in (a).

4.3. Local characterisation of individual particles

For the HA layers in which DND (detonation generated nanodiamond) nanoparticles had been incorporated to improve the mechanical strength [18], it was possible to characterise individual particles at a local level.

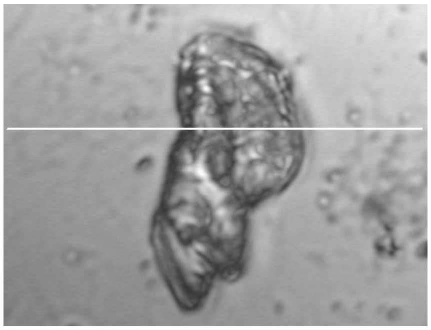

Fig. 8. Extended depth of a field reflection image of a HA-DND particle on a steel substrate (image size 56 µm x 40 µm).

For example, Fig. 8 shows an extended depth of field view of such a particle, made with CPM. An image of a typical XZ view of the fringes at the centre of the particle is shown in Fig. 9(a). The average effective refractive index measured with the technique described in section 2.2 and equation (3) was 1.45.

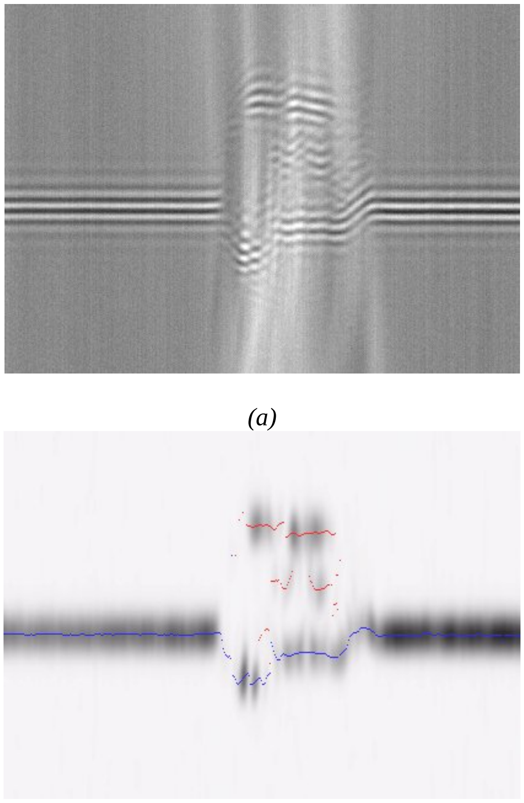

(a)

(b)

Fig. 9. Cross sectional profile from Fig. 8 of the HA-DND particle on a steel substrate after processing: (a) XZ image of raw data (fringes); (b) Processed cross sectional profile from (a)(image size 56 µm x 12 µm).

By processing the XZ image as described in section 2.3, a cross sectional profile of the particle was produced, as shown in Fig. 9(b). The height of the particle was measured to be 3.5 µm. The dark thicker horizontal lines are the fringe envelope profiles. The coloured lines mark the envelope peaks, the blue line corresponding to the substrate surface and the red line to the surface and interior details of the HA-DND particle. These results demonstrate the high axial resolution of this technique for revealing the cross sectional profiles and internal structures of transparent particles.

5. Discussion and conclusions

In this work, we have presented new developments in extended measurement modes of CPM based on white light scanning interferometry. As well as measuring the deep roughness of thick samples, CPM has been extended with the Z-scan technique we have developed for characterising the internal structure of thick complex layers containing several layers or cavities.

Results have been demonstrated on thin layers of DLC deposited on polycarbonate, in which as well as quantified analysis of delaminating "bubbling" effects of thin layers of DLC, useful information was also revealed concerning the variation in adherence under different growth conditions. Other results have been demonstrated on the roughness characterisation of thick layers of hydroxyapatite (<30 µm), as well as the analysis of the internal structure (buried transparent layers, cavities…). Individual DND particles incorporated in HA have been characterised, providing measurements of the local effective refractive index and cross sectional profiles.

Future work is under way for developing simulation software for modelling the response of the optical probe in the presence of single and multiple layers. The results of such simulations will be useful in developing more advanced signal processing techniques for improving the cross sectional profiles. We have thus demonstrated the capability of using CPM as a potential technique for performing high resolution tomography on complex transparent and semi-translucent layers.

Acknowledgements

This work was supported by the InESS Laboratory (Strasbourg) and the INTERREG III Regional-European programme. Thanks are extended to Tom Heiser for useful discussions and to Luc Hébrard for providing the CMOS chip. Support is also acknowledged of two Bulgarian national projects: with the Ministry of Education and Science, Bulgaria (No: TK-X 1708/2007) and the Agency of Innovation, Bulgaria (02-54/2007). The support of a NATO grant CBP.EAP.RIG.982693 is acknowledged.

References

[1] E. Pecheva, P. Montgomery, D. Montaner, L. Pramatarova, Langmuir **23**, 3912 (2007).
[2] P.C. Montgomery, Nanotechnology **1**, 54 (1990).
[3] P. C. Montgomery, A. Benatmane, E. Fogarassy, J. P. Ponpon, Materials Science and Engineering **B91-92**, 79 (2002).
[4] A. Benatmane, P. Montgomery, E. Fogarassy, D. Zahorsky, Appl. Surf. Sci. **208-209**, 189 (2003).
[5] P. Montgomery, D. Montaner, O. Manzardo, M. Flury, H.P. Herzig, Thin Sol. Films **450**, 79 (2004).
[6] A. Benatmane, P. Montgomery, Eur. Phys. J. – Appl. Phys. **27**, 411 (2004).
[7] E. Pecheva, P. C. Montgomery, D. Montaner, L. Pramatarova, Z. Zanev, SPIE **6341**, 634137 (2006).
[8] S. Petitgrand, Ph.D. thesis, Université Paris-Sud XI, Institut d'Electronique Fondamentale, Orsay, France, 29 September 2005.
[9] P. C. Montgomery, C. Draman, M. Sieskind, J. P. Ponpon, Phys. Stat. Sol. (c) **0**, 3, 1044 (2003).
[10] P. C. Montgomery, F. Anstotz, G. Johnson, R. Kiefer, Journal of Materials Science: Materials in Electronics, accepted for publication, 2008.
[11] M. C. Park, S. W. Kim, Optics letters **26**, 420 (2001).
[12] P. C. Montgomery, D. Montaner, O. Manzardo, H. P. Herzig, SPIE **5458**, 34 (2004).
[13] Q. Zhan, J. R. Leger, Applied Optics **41**, 22, 4443 (2002).
[14] A. Golanski, D. Grambole, J. Hommet, F. Herrman, P. Kern, L. McDonnell, F. Piazza, J. P. Stoquert, Mater. Res. Soc. Symp. Proc. **675**, pp. W12.2.1 (2001).
[15] M. Flury, A. Benatmane, P. Gérard, P. C. Montgomery, J. Fontaine, T. Engel, J. P. Schunck, Optical Engineering **41**, pp. 10, 2407, (2002).
[16] O. Tuzun, J. M. Auger, I. Gordon, A. Focsa, P. C. Montgomery, C. Maurice, G. Beaucarne, A. Slaoui, J. Poortmans, Thin Solid Films **516**, 6882 (2008).
[17] E. Pecheva, T. Petrov, C. Lungu, P. Montgomery, L. Pramatarova, Chem. Eng. J. **137**, 144-153 (2008).
[18] L. Pramatarova, E. Pecheva, S. Stavrev, T. Spasov, P.C. Montgomery, A. Toth, M. Dimitrova, M. Apostalova, J. Optoelec. & Adv. Mat. **9**, 236 (2007).

---

[*] Corresponding author: paul.montgomery@iness.c-strasbourg.fr